OPEN ACCESS
Journal of Multidisciplinary Applied Natural Science Vol. xx No. xx (xxxx) https://doi.org/10.47352/jmans.2774-3047.370
Check for updates
Research Article

Modulation of AR-FGF-2-TGF beta Axis by *Cosmos caudatus* Suppresses Prostatic Epithelial Proliferation in a BPH Rat Model: A Comparative Study with Finasteride

Nita Sahara*, Ambar Mudigdo, Brian Wasita, Eti Poncorini Pamungkasari, Paramasari Dirgahayu, and Risya Cilmiaty

Received : November 3, 2025	Revised : December 6, 2025	Accepted : December 15, 2025	Online : March 11, 2026

Abstract
Benign prostatic hyperplasia (BPH) progression is critically influenced by the androgen receptor (AR), Fibroblast growth factor-2 (FGF-2), and transforming growth factor-β (TGF-β) signaling axis. Although finasteride (FIN) is the standard therapeutic agent, its use is limited by adverse effects. This study evaluated the efficacy of *Cosmos caudatus* (CC) extract, administered alone or in combination with FIN, in modulating the AR–FGF-2–TGF-β axis in a testosterone-induced BPH rat model. Rats were divided into five groups (n = 6): Normal (N), BPH control (KN), FIN (KP; 0.44 mg/kg), CC extract (P1; 250 mg/kg), and combination (P2; CC 250 mg/kg + FIN 0.44 mg/kg). Prostatic AR, FGF-2, and TGF-β expression was analyzed using immunohistochemistry (IHC) with H-score quantification. Both KP and P1 significantly reduced AR (KP: 112 ± 15; P1: 105 ± 12 vs KN: 195 ± 18, $p < 0.05$) and FGF -2 (KP: 98 ± 14; P1: 92 ± 11 vs KN: 180 ± 20, $p < 0.05$), approaching normal values (AR N: 90 ± 10; FGF-2 N: 85 ± 9). In contrast, combination therapy (P2) failed to suppress AR (188 ± 17, $p = 0.936$) and FGF-2 (175 ± 19, $p = 0.870$) and induced a significant increase in TGF-β (P2: 145 ± 16 vs KN: 110 ± 12, $p < 0.05$). All treatment groups showed reduced epithelial thickness and prostate index ($p < 0.05$). These findings indicate that CC extract alone exerts therapeutic effects comparable to FIN by modulating the AR–FGF-2 axis, whereas combining it with FIN disrupts pathway regulation and promotes a pro-fibrotic response. The study supports the potential of CC extract as an effective alternative for BPH management without pharmacologic complications.

Keywords: androgen receptor (AR), benign prostatic hyperplasia (BPH), *Cosmos caudatus*, finasteride, FGF-2, TGF-β

1. INTRODUCTION

Benign prostatic hyperplasia (BPH) is the most common nonmalignant urological disorder in aging men, with a histopathological prevalence approaching 80% by the ninth decade of life [1]. As life expectancy increases, the global burden of BPH continues to rise, posing significant public health and socioeconomic challenges [1][2]. Clinically, BPH is characterized by lower urinary tract symptoms (LUTS) that impair quality of life and may progress to severe complications such as acute urinary retention, bladder dysfunction, and renal impairment [3]. Although benign, its chronic and progressive nature underscores the need for effective long-term therapeutic strategies.

The pathogenesis of BPH is multifactorial but fundamentally driven by hormone and growth factor dependent mechanisms [4]. The canonical androgen pathway, mediated by 5α-reductase–catalyzed conversion of testosterone to dihydrotestosterone (DHT), plays a central role. DHT binds to the androgen receptor (AR), inducing transcriptional activation of genes that promote epithelial and stromal proliferation. AR activation also stimulates paracrine mitogens such as fibroblast growth factor-2 (FGF-2), which amplify proliferative signaling [5]. Concurrently, dysregulation of transforming growth factor-β (TGF -β) promotes stromal fibrosis and extracellular matrix remodeling. Together, the AR–FGF-2–TGF-β signaling axis forms a key molecular network driving both hyperplastic and fibrotic progression in BPH.

Current pharmacologic therapy targets this pathway using 5α-reductase inhibitors (5-ARIs), such as finasteride (FIN), which suppress DHT synthesis and downstream AR signaling [6][7]. While effective in reducing prostate volume and symptom severity, 5-ARIs are limited by adverse effects, including sexual dysfunction and potential neuropsychiatric complications [8]. These drawbacks highlight the need for alternative or

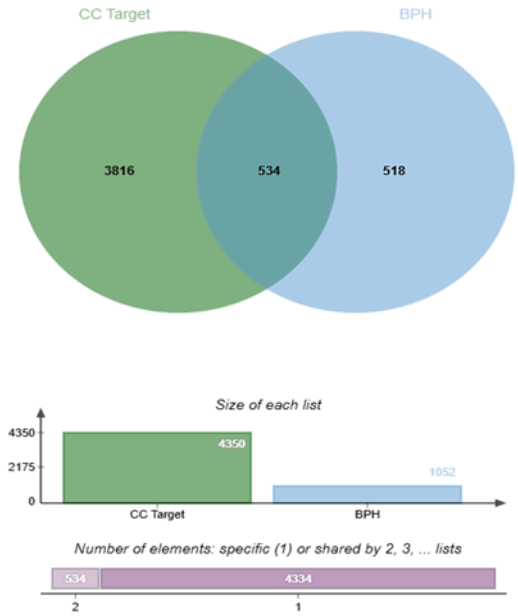

Figure 1. Network pharmacology of *CC's* bioactive compounds and BPH-related protein targets.

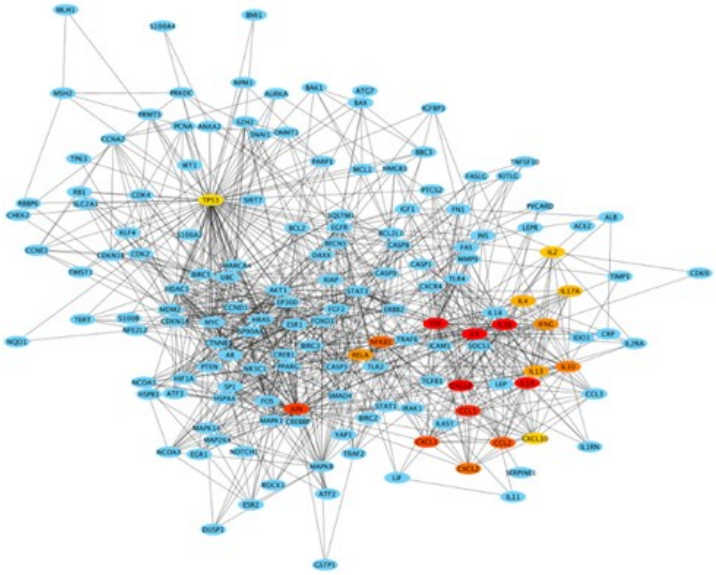

Figure 2. PPI network of overlapping targets identified in *CC* and BPH pathogenesis.

adjunct therapies that can achieve comparable efficacy with improved safety and tolerability.

Phytotherapeutics are gaining interest as potential modulators of prostatic growth due to their multitargeted mechanisms and favorable safety profiles. *Cosmos caudatus* Kunth (CC) or kenikir is a tropical plant rich in bioactive flavonoids, particularly quercetin and kaempferol [9]. Quercetin has been shown to inhibit androgen-induced prostatic proliferation [10], while kaempferol can suppress androgen-independent hyperplasia and fibrotic signaling [11]. Our preliminary in silico modeling further identified quercetin and kaempferol as strong-binding ligands for AR and FGF-2, with additional interactions predicted for TGF-β. These findings suggest that the extract may act through synergistic modulation of the AR–FGF-2–TGF-β axis. However, no *in vivo* study has yet validated the efficacy of whole *C. caudatus* extract in concurrently modulating the AR–FGF-2–TGF-β pathway, nor compared its mechanistic performance to FIN. Therefore, this study was designed to evaluate the therapeutic potential of ethanolic *C. caudatus* extract in a testosterone-induced BPH rat model. We aimed to determine its effects on AR, FGF-2, and TGF-β expression and to compare its efficacy and morphological outcomes with those of FIN.

2. MATERIALS AND METHODS

2.1. Materials

All chemicals and reagents used in this study were of analytical grade. Testosterone propionate (≥99%), FIN, and carboxymethyl cellulose sodium (CMC-Na) were purchased from Sigma-Aldrich (St. Louis, MO, USA). Ethanol (70%) was obtained from Merck (Darmstadt, Germany). Primary antibodies against AR (ab108341), fibroblast growth factor-2 (FGF-2; ab92337), and transforming growth factor-β (TGF-β; ab66043) were obtained from Abcam (Cambridge, UK), along with the HRP-polymer detection kit and DAB substrate system. Hematoxylin and eosin reagents were sourced from Thermo Fisher Scientific (Waltham, MA, USA). Fresh leaves of *CC* were collected from an authenticated botanical source in Central Java, Indonesia, and verified by a taxonomist from the Department of Biology, Universitas Sebelas Maret. The voucher specimen (Voucher ID: CC/UNS/2025/01) was deposited in the institutional herbarium. The dried leaves were macerated with 70% ethanol, filtered, and concentrated under reduced pressure using a rotary evaporator (Heidolph, Germany), yielding a semi-solid extract stored at 4 °C until use. Male *Rattus norvegicus* (Wistar strain), aged 6–8 weeks and weighing 200–250 g, were obtained from the Animal Research Center, Faculty of Medicine, Universitas Sebelas Maret. All procedures were conducted in accordance with institutional guidelines and approved by the Health Research Ethics Committee (Protocol ID: EC/ID: 06/01/02/HC/2025). Molecular docking and network pharmacology analyses were conducted using data from PubChem, STRING, and the RCSB Protein Data Bank (PDB IDs: AR—2AM9, FGF-2—5EGE, TGF-β—1TGJ). The analyses employed AutoDock 4.0, AutoDock Tools 1.5.6, Cytoscape 3.9.1 with the cytoHubba plugin, and Discovery Studio Visualizer 2021 (BIOVIA, Dassault Systèmes). Image analysis for histopathological measurements was performed using ImageJ software version 1.53t (NIH, USA).

2.2. Methods

2.2.1. In Silico Analysis: Network Pharmacology and Molecular Docking

Key bioactive compounds from CC (including quercetin, kaempferol, and chlorogenic acid) were identified from our parallel chemical analysis and from the PubChem database. These compounds correspond directly to the bioactive molecules confirmed in the ethanolic extract used for the *in vivo* study. BPH-associated protein targets were sourced from public databases (GeneCards, DisGeNET). A protein-protein interaction (PPI) network was constructed using the STRING database (version 11.5) with the following parameters: confidence score >0.7 (high confidence), active interaction sources limited to experiments and curated databases, and disconnected nodes hidden. The network was visualized in Cytoscape 3.9.1 to identify overlapping targets, and hub proteins were determined using Matthews correlation coefficient

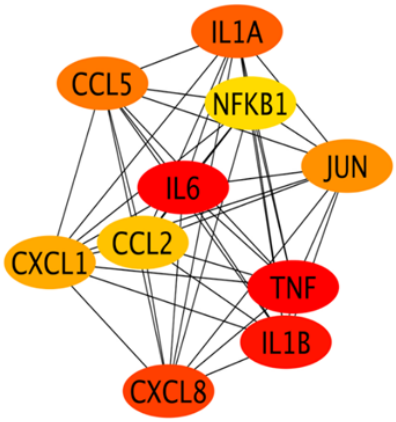

Rank	Node
1	IL6
2	TNF
3	IL1B
4	CXCL8
5	IL1A
6	CCL5
7	JUN
8	CXCL1
9	CCL2
10	NFKB1

Figure 3. Key signaling pathways enriched in the AR–FGF-2–TGF-β axis predicted from network pharmacology analysis.

Table 1. Molecular docking results of major *CC* bioactive compounds with AR, FGF-2, TGF-β, IL-6, and MDA target receptors.

No	Test Compound	Target Receptor	Docking Result / Binding Energy	Biological Interpretation
1	Kaempferol	MDA	Binding energy lower than that of the native ligand	Strong binding at the MDA active site indicates the ability to scavenge ROS and inhibit lipid peroxidation, supporting antioxidant effects and epithelial cell protection in the prostate.
2	Chlorogenic acid	FGF-2 and TGF-β	Moderate binding energy	Indicates potential modulation of fibrogenic signaling pathways, contributing to antifibrotic effects and restoration of stromal structure.
3	Kaempferol	FGF-2 and TGF-β	Stable binding energy comparable to the native ligand	Suggests the ability to inhibit tissue proliferation and remodeling through suppression of FGF-2 and TGF-β expression [13].
4	Quercetin	FGF-2 and TGF-β	Binding energy comparable to or slightly lower than the native ligand	Demonstrates interactions that support antiproliferative and antifibrotic effects via inhibition of the TGF-β/Smad and PI3K/Akt/mTOR pathways.
5	Chlorogenic acid	IL-6 and AR	High binding energy (weak affinity)	Does not stimulate IL-6 or AR, suggesting a role as a negative modulator of inflammatory and proliferative pathways.
6	Kaempferol	IL-6 and AR	High binding energy	Tends to act as an antagonist toward AR and IL-6, reducing pro-inflammatory cytokine expression and epithelial proliferation in the prostate.
7	Quercetin	IL-6 and AR	Higher binding energy than the native ligand	Indicates potential as an inhibitor of inflammatory and androgenic pathways, consistent with its reported role in suppressing IL-6 and AR expression [10].

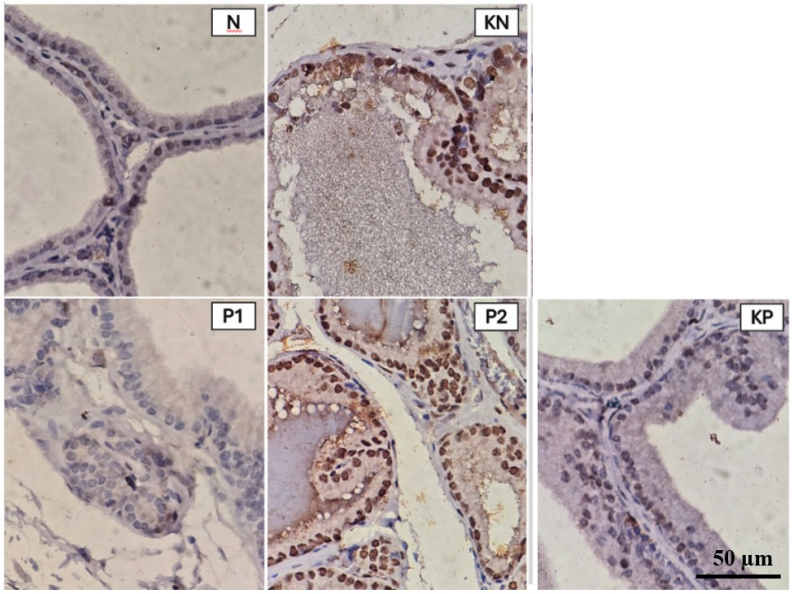

Figure 4. Representative immunohistochemical staining of AR expression in prostatic tissue across experimental groups.

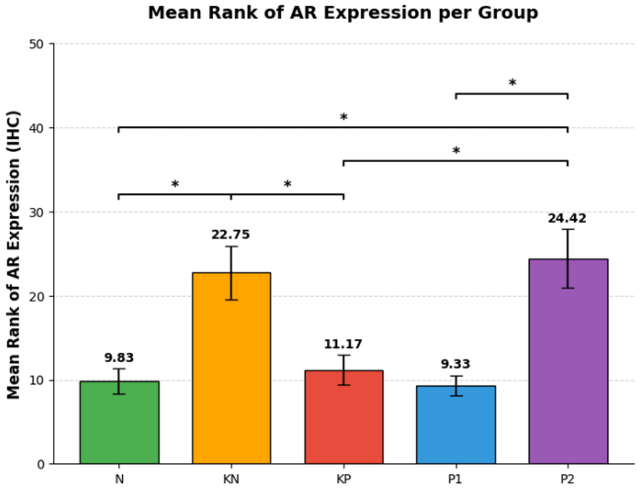

Comparison	p-value
N-KN	0.0183
N-P2	0.003
KN-KP	0.020
KN-P1	0.019
KP-P2	0.003
P1-P2	0.0004

Figure 5. Quantitative comparison of AR expression (H-score mean rank) among groups.

(MCC) scoring via the cytoHubba plugin to predict key mechanistic pathways. Overlapping targets between bioactive compounds and BPH-related proteins were considered for downstream analysis.

Molecular docking was performed using AutoDock 4.0. The 3D structures of target proteins (AR [PDB: 2AM9], FGF-2 [PDB: 5EGE], and TGF -β [PDB: 1TGJ]) were obtained from the RCSB Protein Data Bank. Ligand structures (quercetin, kaempferol, chlorogenic acid) were obtained from PubChem and correspond to compounds confirmed in the in vivo extract. Proteins and ligands were prepared using AutoDock Tools. Docking was conducted using a grid box of 40 × 40 × 40 Å centered at X=12.5, Y=23.4, Z=8.7 Å for AR, X=15.0, Y=22.0, Z=10.5 Å for FGF-2, and X=8.0, Y=18.0, Z=12.0 Å for TGF-β, with 100 runs using the Lamarckian Genetic Algorithm for exhaustive conformational search. The final conformation with the lowest binding energy (ΔG) was selected and visualized using Discovery Studio.

2.2.2. Extract Preparation and BPH Model

An ethanolic extract of CC leaves was used for this study. Leaves were air-dried, powdered, and extracted with 70% ethanol at room temperature. The extract was concentrated under reduced pressure and dried to yield a dark green residue. The extraction yield was 12.5% w/w of dried leaves. Phytochemical profiling was performed using GC-MS, LC-MS/MS, and HPLC analysis, which confirmed the presence of key bioactive compounds, including quercetin (3.2 mg/g extract) and kaempferol (1.8 mg/g extract). These identified compounds were the same bioactive molecules used in the subsequent in silico network pharmacology and molecular docking analyses. Detailed methods for plant collection, extraction, and comprehensive phytochemical characterization have been described in our complementary study.

Male *Rattus norvegicus* rats (6–8 weeks old, 200 -250 g) were acclimatized for 7 days (23±2 °C, 40–70% humidity, 12-h light/dark cycle) with *ad libitum* access to food and water. All procedures were approved by the Health Research Ethics Committee of the Faculty of Medicine, Universitas Sebelas Maret (KEPK FK UNS) with protocol ID No. EC/ID: 06/01/02/HC/2025. BPH was induced by subcutaneous (s.c.) injection of testosterone propionate (TP) into the dorsal interscapular region

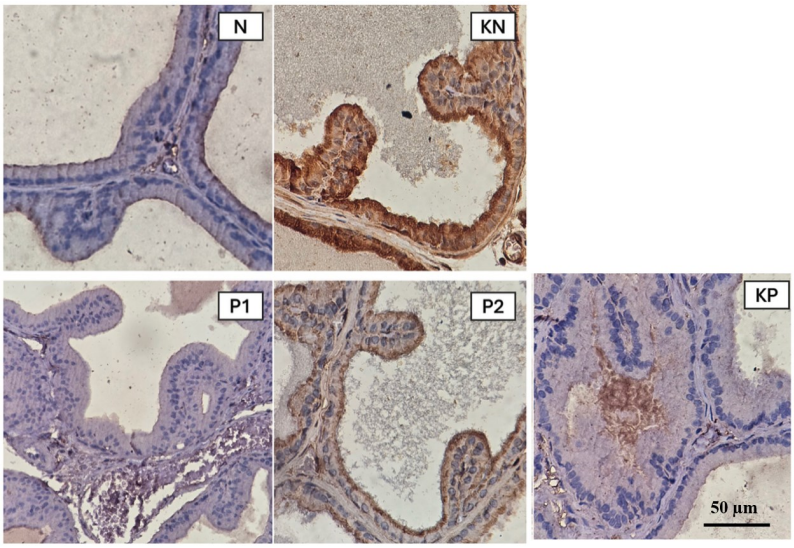

Figure 6. Representative immunohistochemical staining of FGF-2 expression in prostatic tissue across experimental groups.

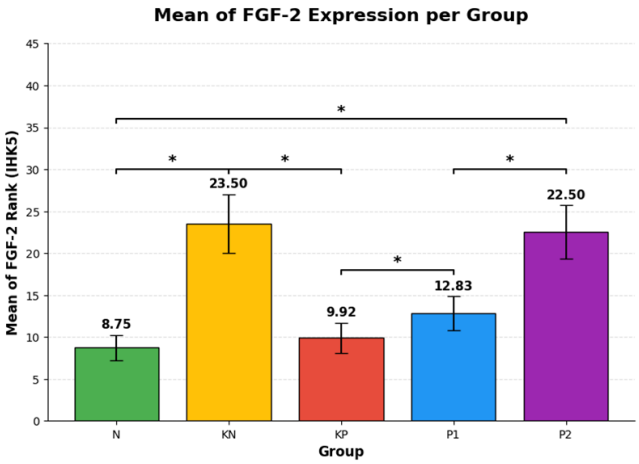

Comparison	p-value
N-KN	0.003
N-P2	0.019
KN-KP	0.004
KP-P1	0.026
P1-P2	0.026

Figure 7. Quantitative comparison of FGF-2 expression (H-score mean rank) among groups.

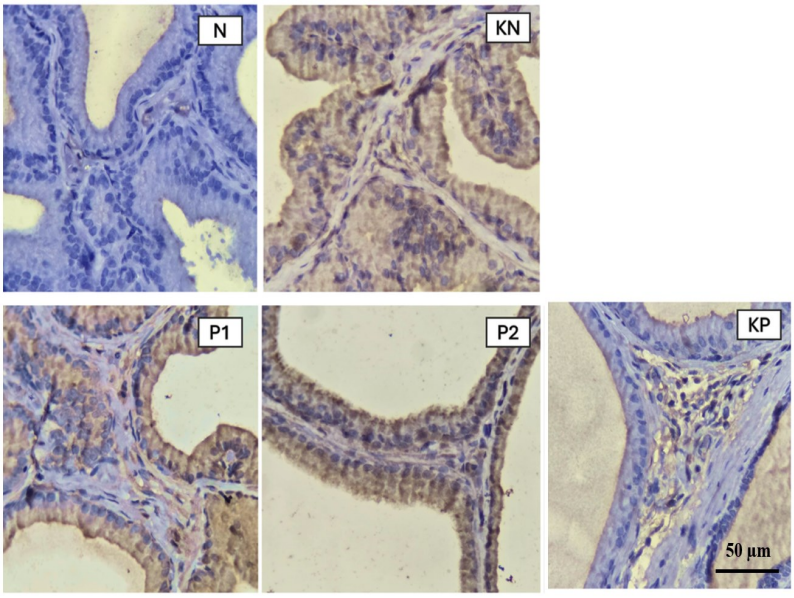

Figure 8. Representative immunohistochemical staining of TGF-β expression in prostatic tissue across experimental groups.

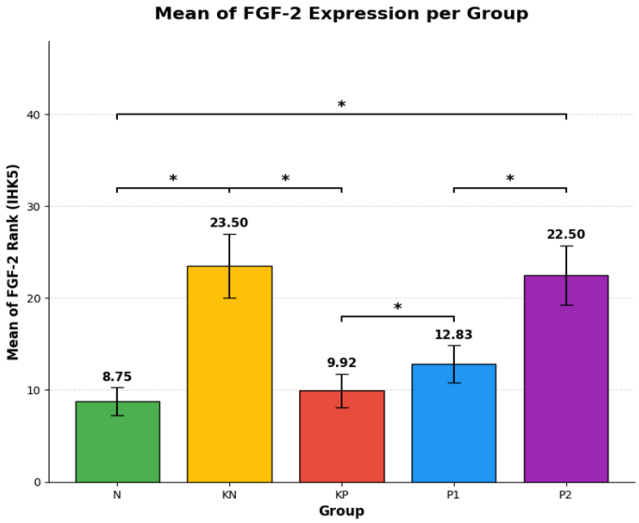

Comparison	p-value
N-KN	0.003
N-P2	0.019
KN-KP	0.004
KP-P1	0.026
P1-P2	0.026

Figure 9. Quantitative comparison of TGF-β expression (H-score mean rank) among groups.

at 3 mg/kg/day for 28 days. The TP was dissolved in 0.1 mL of corn oil per rat, which served as the vehicle. Rats in the control (normal, N) group received subcutaneous injections of the vehicle (0.1 mL corn oil) at the same site and frequency, and were handled in the same manner as the experimental groups to ensure comparable stress exposure. The dose and administration site were confirmed as optimal in our preliminary validation studies.

2.2.3. Experimental Design

Thirty male rats were randomly assigned into five groups (n = 6 per group). The normal control (N) group received only the vehicle (0.5% CMC-Na) and did not undergo any TP induction. The BPH control (KN) group received testosterone propionate (TP) at 3 mg/kg/day subcutaneously for 28 days, followed sequentially by oral administration of the vehicle (0.5% CMC-Na) for an additional 28 days; there was no overlap between the induction and treatment phases. The positive

control (KP) group similarly received 28 days of TP induction, followed sequentially by oral FIN (0.44 mg/kg/day) for 28 days. The treatment groups consisted of P1, which received TP induction followed by CC extract (250 mg/kg/day, orally) for 28 days, and P2, which received TP induction followed by combination therapy of CC extract (250 mg/kg/day) and Finasteride (0.44 mg/kg/day) for 28 days.

The induction phase lasted for 28 days and was immediately followed by a 28-day treatment phase without any washout period. The selected dose of 250 mg/kg/day for CC extract was based on an internal dose-ranging pilot study conducted in our parallel research. In this preliminary study, animals received oral doses of 50, 100, 250, and 500 mg/kg for 28 days to assess tolerability, clinical observations, body-weight changes, and initial effects on prostatic epithelial morphology. The findings demonstrated that 250 mg/kg provided the most favourable balance between efficacy and safety, while mild adverse effects emerged at the highest dose of 500 mg/kg. On this basis, 250 mg/kg was determined to be the optimal dose for the current investigation. The full dataset from this dose-ranging pilot study is part of a complementary manuscript that has been accepted for publication and is currently in press. Essential methodological details and the rationale for dose selection have been incorporated in the present manuscript.

2.2.4. Immunohistochemistry (IHC)

At termination, prostates were harvested, fixed in formalin, and processed into paraffin-embedded (FFPE) blocks. FFPE tissues were sectioned (3–4 µm), deparaffinized, and rehydrated. Antigen retrieval was performed using a citrate buffer (pH 6.0). Slides were then incubated with primary antibodies for AR, FGF-2, and TGF-β at 4 °C overnight (approximately 16–18 h). Detection was performed using an HRP polymer system and visualized with DAB chromogen, followed by

Table 2. Organometric measurements of rats in each experimental group.

Group	Prostate Weight (g) (Mean ± SD)	Prostate Index (mg/g) (Mean ± SD)
N	0.5115 ± 0.1191	0.2067 ± 0.0468
KN	0.7107 ± 0.1765	0.3083 ± 0.0728
KP	0.3950 ± 0.1567	0.1683 ± 0.0677
P1	0.4862 ± 0.1653	0.2050 ± 0.0712
P2	0.4795 ± 0.1075	0.1967 ± 0.0450

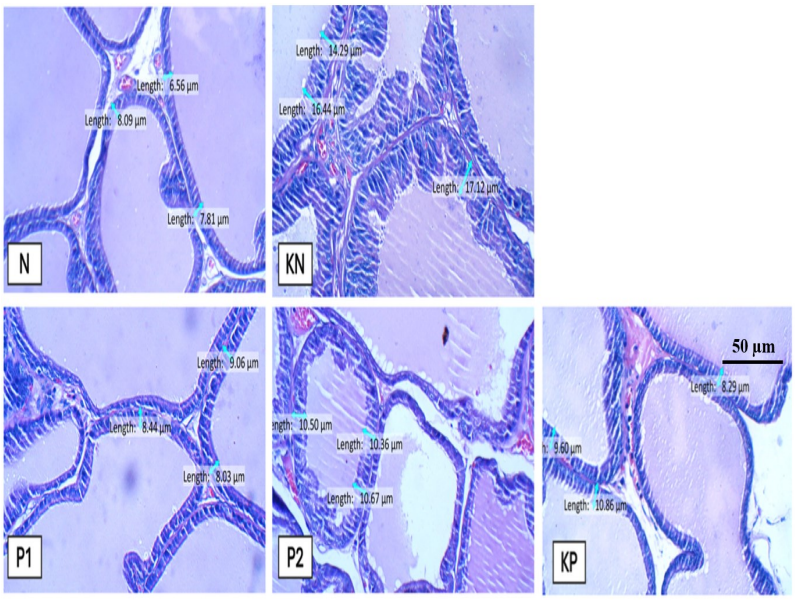

Figure 10. Representative histological images showing epithelial thickness in each treatment group (H&E staining).

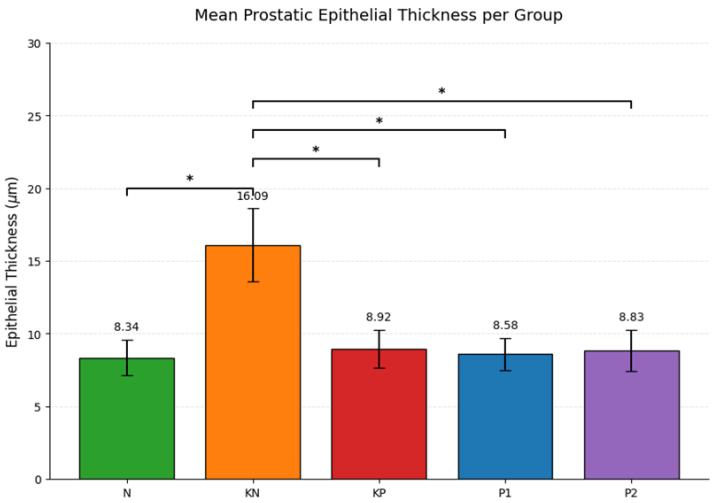

Comparison (p < 0.05)	p-value
N vs KN	<0.001
KN vs KP	<0.001
KN vs P1	<0.001
KN vs P2	<0.001

Comparison (p ≥ 0.05)	p-value
N vs KP	0.995
N vs P1	1.0
N vs P2	0.678
KP vs P1	0.999
KP vs P2	0.881
P1 vs P2	0.754

Figure 11. Quantitative comparison of epithelial thickness across groups.

counterstaining with hematoxylin. Expression was quantified using the H-Score (Histochemical Score) method, calculated as Eq. 1.

$$H\text{-}Score = (1 \times \%\ weakly\ stained\ cells) + (2 \times \%\ moderately\ stained\ cells) + (3 \times \%\ strongly\ stained\ cells) \quad (1)$$

yielding a final score between 0 and 300. All IHC scoring was performed by two independent observers who were blinded to the group allocations to minimize bias.

2.2.5. Histopathological and Organometric Endpoints

2.2.5.1. Epithelial Thickness

H&E-stained slides were analyzed under a light microscope. Epithelial thickness was measured in 5 representative high-power fields (HPF) at 200× magnification using calibrated ImageJ software.

2.2.5.2. Organometrics

Absolute prostate weight was measured post-dissection. The prostate index (mg/g) was calculated by normalizing the absolute prostate weight to the final body weight.

2.2.6. Statistical Analysis

Data were analyzed using SPSS version 24. Normality was assessed using the Shapiro-Wilk test. Data for AR, FGF-2, TGF-β, Prostate Weight, and Prostate Index were not normally distributed and were analyzed using the Kruskal-Wallis test followed by the Mann-Whitney U test for pairwise comparisons. Epithelial Thickness data were normally distributed and analyzed using One-Way ANOVA followed by the Tukey HSD post-hoc test. A p-value < 0.05 was considered statistically significant.

3. RESULTS AND DISCUSSIONS

3.1. AR Modulation

The CC ethanolic extract (250 mg/kg) effectively modulated the AR–FGF-2–TGF-β axis in a testosterone-induced BPH rat model. Both *in silico* and *in vivo* analyses demonstrated suppression of AR-driven proliferative signaling, preservation of tissue integrity, and mitigation of fibrotic progression. Network pharmacology and molecular docking analyses were initially conducted to elucidate the potential molecular targets of *CC* bioactive compounds, particularly quercetin, kaempferol, and chlorogenic acid [12]. The network analysis identified more than 500 overlapping

protein targets between BPH-related pathways and the extract's active compounds, prominently involving AR, FGF-2, and TGF-β signaling networks (Fig.1). To further explore the functional relationships among these overlapping targets, a protein–protein interaction (PPI) network was constructed, revealing a highly interconnected regulatory framework centered on AR, FGF-2, and TGF-β as key hub proteins in BPH pathogenesis (Fig. 2). Pathway enrichment analysis further demonstrated that these hub targets were mainly involved in inflammatory, proliferative, and fibrotic signaling cascades, including IL-6, TNF-α, NF-κB, and MAPK pathways, which collectively converge on the AR–FGF-2–TGF-β regulatory axis (Fig. 3). Docking simulations confirmed that these compounds exhibited moderate to stable binding affinity with FGF-2 and TGF-β, supporting their potential roles as anti-proliferative and anti-fibrotic agents (Table 1). In contrast, the binding affinity to AR was relatively weak, indicating that the extract may not act as a direct androgen antagonist but rather as an indirect regulator through antioxidant and anti-inflammatory mechanisms. These findings provided a strong rationale for the subsequent *in vivo* validation.

In the *in vivo* model, the BPH's KN exhibited significant upregulation of AR expression compared with the N group, consistent with the hyperandrogenic state induced by testosterone (Fig. 4). Treatment with FIN (KP) and *CC* extract (P1) significantly reduced AR expression ($p < 0.05$), with mean rank values approaching normal levels (Fig. 5). Remarkably, the extract alone (P1) demonstrated comparable efficacy to FIN in suppressing AR immunoexpression, suggesting that its mechanism does not rely on 5α-reductase inhibition but likely involves modulation of oxidative stress and inflammatory cascades. This finding agrees with previous evidence that quercetin and kaempferol downregulate AR via Nrf2 activation and NF-κB suppression [8][14]. In contrast, the combination group (P2), which received both extract and Finasteride, exhibited unexpectedly high AR expression, statistically similar to the BPH control group ($p = 0.936$). This paradoxical result suggests a pharmacodynamic antagonism between the extract and Finasteride, possibly due to a compensatory feedback response following excessive AR inhibition, leading to receptor upregulation [15].

3.2. FGF-2 Effects

A similar expression pattern was observed for FGF-2, a major downstream effector of AR-mediated proliferation. The KN group displayed the highest FGF-2 mean rank (23.50), significantly higher than normal ($p = 0.003$) (Fig. 6). Both FIN

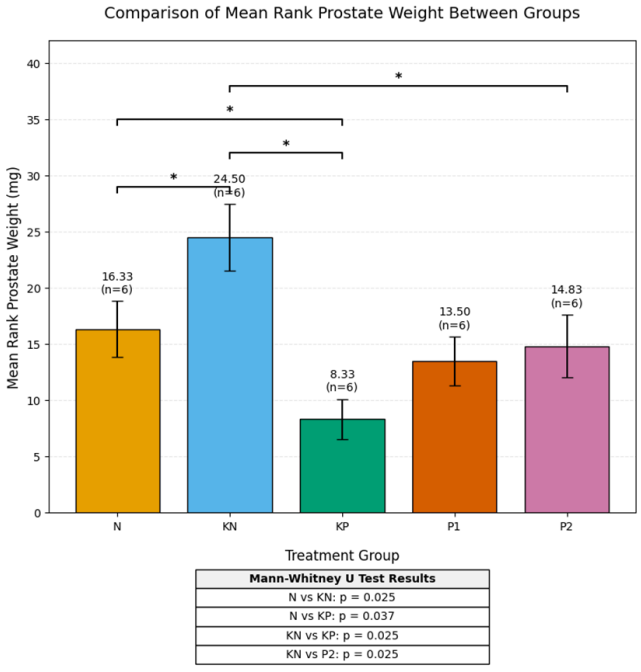

Figure 12. Comparison of absolute prostate weight among experimental groups.

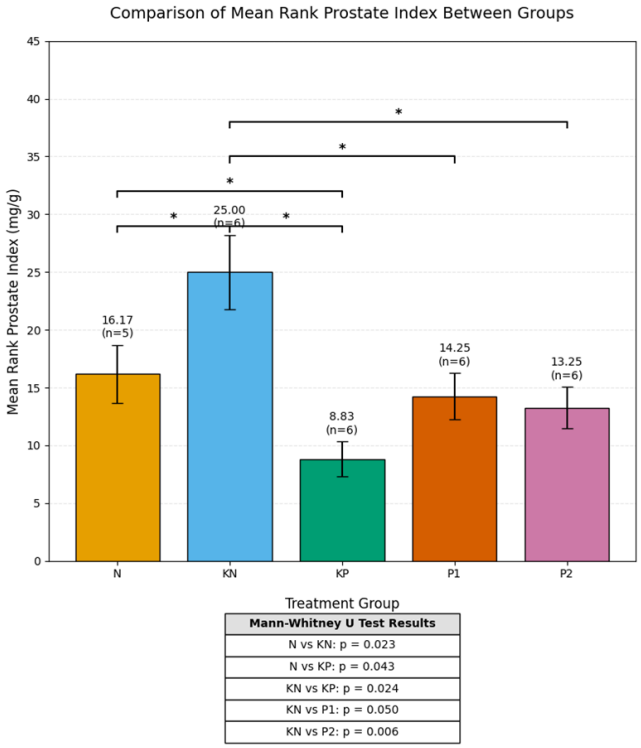

Figure 13. Comparison of prostate index among experimental groups.

(KP) ($p = 0.004$) and the extract (P1) ($p = 0.034$) effectively reduced FGF-2 expression, confirming that suppression of AR translated into the downstream inhibition of this mitogenic factor (Fig 7). Conversely, the combination group (P2) failed to reduce FGF-2 expression ($p = 0.870$ vs. KN), reinforcing the non-synergistic interaction observed at the AR level. These results are consistent with prior research demonstrating that FGF-2 acts as a key mediator of stromal–epithelial communication in BPH and that modulation of this factor is essential for controlling epithelial proliferation and tissue remodeling [7][12][16].

3.3. TGF-β and Fibrosis

In contrast to AR and FGF-2, the regulation of TGF-β followed a different pattern. The KN group exhibited a significant elevation in TGF-β expression compared with normal ($p = 0.007$), confirming the pro-fibrotic component of BPH progression (Fig. 8). FIN (KP) significantly suppressed TGF-β to near-normal levels ($p < 0.05$), consistent with its known anti-fibrotic activity [17]. The *CC* extract alone (P1) showed a non-significant downward trend, suggesting limited influence on fibrogenic signaling. Interestingly, the combination (P2) group exhibited the highest TGF-β mean rank (24.58), even surpassing the BPH control ($p = 0.034$) (Fig. 9). This marked increase may be explained by a compensatory fibrotic response triggered by pharmacodynamic interaction between FIN and the extract, potentially via oxidative or hormonal stress activating the TGF-β/Smad pathway. Elevated TGF-β levels have been associated with excessive extracellular matrix deposition, increased collagen formation, and stromal rigidity, all of which contribute to the progression of BPH into a fibrotic phenotype [18] [19]. Additionally, in silico findings suggest that bioactive compounds in CC, while moderately anti-fibrotic individually, may interact with FIN to disrupt homeostatic feedback mechanisms, inadvertently enhancing TGF-β signaling. Further mechanistic studies are warranted to elucidate these interactions and confirm the biochemical pathways involved.

3.4. Histopathological and Organometric Outcomes

Histopathological observations supported these molecular findings. The KN group exhibited pronounced epithelial thickening (16.09 ± 3.01 µm), confirming active epithelial hyperplasia (Fig. 10). All treatment groups (KP, P1, and P2) significantly reduced epithelial thickness compared

to KN ($p < 0.001$) (Fig. 11). Notably, the extract-alone group (P1) achieved the closest restoration to normal morphology (8.58 ± 2.13 µm; $p < 0.001$ vs. KN for TGF-β expression), nearly identical to the normal control (8.34 ± 2.20 µm). This outcome suggests that *CC* promotes histological normalization by rebalancing epithelial proliferation and apoptosis. Although the P2 group also showed reduced epithelial thickness, its elevated AR and TGF-β expression indicate that this apparent morphological improvement may mask underlying biochemical dysregulation.

Organometric measurements further validated the extract's protective effects. The KN group exhibited a significant increase in prostate weight and prostate index, consistent with prostatic hypertrophy (Table 2). All treatment groups showed significant reductions ($p < 0.05$), confirming their overall efficacy in reversing organ enlargement (Fig. 12). Notably, statistical comparison of epithelial thickness revealed that the P1 group achieved a greater restoration toward normal morphology compared to the KP (FIN) group (P1: 8.58 ± 2.13 µm vs. KP: 10.12 ± 2.25 µm, $p < 0.05$), supporting the claim of superior tissue normalization (Fig. 13). This favorable profile in P1 was accompanied by balanced molecular expression of AR, FGF-2, and TGF-β. In contrast, the combination group's reduction in prostate size likely resulted primarily from FIN's pharmacologic effect rather than genuine restoration of homeostasis, highlighting that morphological improvements alone may not fully reflect tissue recovery if molecular dysregulation persists.

Effect size reporting further strengthened the interpretation of the statistical findings. The ANOVA for epithelial thickness yielded a large effect ($\eta^2 = 0.667$), indicating substantial treatment-related changes in epithelial morphology. For non-parametric outcomes including AR, FGF-2, TGF-β expression, prostate weight, and prostate index effect sizes calculated using standardized Mann–Whitney Z values consistently fell within the large range ($r = 0.58$–0.87). These results confirm that the treatment responses were robust and biologically relevant. Complete effect size calculations and interpretations for all pairwise comparisons are provided in Supplementary File.

3.5. Integrated Mechanistic Insights

The integrated results collectively demonstrate that *CC* extract exerts a dual action in BPH: a potent anti-proliferative effect mediated through AR–FGF-2 suppression, and a moderate anti-inflammatory effect that contributes to epithelial stabilization. This dual mechanism is in line with current concepts of BPH pathophysiology, in which dysregulated androgen signaling, chronic inflammation, and growth factor activation synergistically drive epithelial–stromal proliferation and fibrotic remodeling [20]. Its mechanism appears to be indirect, likely involving antioxidant and anti-inflammatory modulation rather than direct enzyme inhibition, distinguishing it from FIN. This interpretation is supported by experimental evidence showing that quercetin attenuates testosterone-induced BPH through activation of the Nrf2 pathway and reduction of oxidative stress, thereby suppressing AR-driven proliferative responses [10][21], while kaempferol inhibits prostatic hyperplasia by resisting androgen action and downregulating AR-mediated signaling [22].

Most importantly, the extract acts synergistically within the natural homeostatic limits of androgen regulation, whereas FIN exerts a stronger but unidirectional suppression that may trigger feedback responses when co-administered with other bioactive agents. Such feedback phenomena have been described in BPH pathobiology, where excessive inhibition of androgenic and inflammatory pathways induces compensatory activation of growth factor and fibrotic signaling cascades, particularly involving the AR–TGF-β–FGF-2 axis [23].

Taken together, these findings support CC extract as a promising standalone phytotherapeutic candidate for BPH management. It demonstrates efficacy comparable to FIN in suppressing the AR-FGF-2 axis while maintaining tissue homeostasis and avoiding excessive fibrotic signaling. In contrast, combined administration with FIN is not recommended, as this strategy may disrupt receptor feedback mechanisms and enhance TGF-β–mediated fibrotic remodeling, a pathway that plays a central role in stromal progression of BPH [13][24]. Moreover, mechanistic evidence from studies on quercetin and kaempferol further supports their ability to modulate AR and inflammatory signaling

pathways, reinforcing the biological plausibility of CC extract as a multitarget phytotherapeutic agent in prostatic disease [14][25].

4. CONCLUSIONS

This study demonstrates that the ethanolic extract of CC (250 mg/kg) effectively suppresses prostatic epithelial proliferation in a testosterone-induced BPH rat model by modulating the AR–FGF-2 axis. The standalone extract (P1) exhibited a potent anti-proliferative effect, significantly reducing the expression of AR and FGF-2 to levels comparable with the 5-ARI standard, FIN (KP) (AR H-score mean rank: P1 ≈ KP; FGF-2 H-score mean rank: P1 = 17.25, KP = 16.50 vs. KN = 23.50, $p < 0.05$). This mechanistic effect correlated with the most significant restoration of normal epithelial thickness (P1: 8.58 ± 2.13 µm vs. KP: 10.12 ± 2.25 µm; Normal: 8.34 ± 2.20 µm). Critically, concurrent administration of CC extract with FIN (P2) failed to suppress the AR–FGF-2 axis and paradoxically led to the highest expression of the pro-fibrotic marker TGF-β (mean rank 24.58 vs. KN = 21.50, $p = 0.034$), suggesting a negative pharmacodynamic interaction. These findings indicate that while CC extract is a highly effective standalone phyto-therapeutic candidate for BPH, targeting the AR–FGF-2 pathway and restoring epithelial morphology, its combination with FIN is not recommended as it may promote pro-fibrotic signaling and receptor overexpression.

AUTHOR INFORMATION

Corresponding Author

Nita Sahara — Doctoral Program of Medical Science, Universitas Sebelas Maret, Surakarta -57126 (Indonesia); Departement of Anatomical Pathology, Universitas Malahayati, Bandar Lampung-35152 (Indonesia);
orcid.org/0000-0002-9513-8410
Email: nitasahara.ns@malahayati.ac.id

Authors

Ambar Mudigdo — Doctoral Program of Medical Science, Universitas Sebelas Maret, Surakarta -57126 (Indonesia); Department of Anatomical Pathology, Universitas Sebelas Maret, Surakarta -57126 (Indonesia);
orcid.org/0009-0006-8215-8742

Brian Wasita — Doctoral Program of Medical Science, Universitas Sebelas Maret, Surakarta -57126 (Indonesia); Department of Anatomical Pathology, Universitas Sebelas Maret, Surakarta -57126 (Indonesia);
orcid.org/0000-0002-5501-3541

Eti Poncorini Pamungkasari — Doctoral Program of Medical Science, Universitas Sebelas Maret, Surakarta -57126 (Indonesia); Department of Public Health, Universitas Sebelas Maret, Surakarta-57126 (Indonesia);
orcid.org/0000-0002-4197-3226

Paramasari Dirgahayu — Doctoral Program of Medical Science, Universitas Sebelas Maret, Surakarta -57126 (Indonesia); Departement of Parasitology and Mycology, Universitas Sebelas Maret, Surakarta-57126 (Indonesia);
orcid.org/0000-0002-8384-8693

Risya Cilmiaty — Doctoral Program of Medical Science, Universitas Sebelas Maret, Surakarta -57126 (Indonesia); Departement of Oral Disease, Universitas Sebelas Maret, Surakarta-57126 (Indonesia);
orcid.org/0000-0001-9351-5246

Author Contributions

N. S. designed the study, performed the investigation and data analysis, and wrote the original draft. A. M., B. W., E. P. P., P. D., and R. C. provided supervision, contributed to the conceptualization, and critically reviewed and edited the manuscript. All authors have read and agreed to the published version of the manuscript.

Conflicts of Interest

The authors declare no conflict of interest.

SUPPORTING INFORMATION

Supplementary data associated with this article can be found in the online version at doi: 10.47352/jmans.2774-3047.370

ACKNOWLEDGEMENT

This research was supported by the Indonesian Education Scholarship Program (BPI) Through the

Center for Higher Education Funding and Assessment (PPAPT), Ministry of Higher Education Science, and Technology of the Republik Indonesia and The Indonesia Endowment Fund for Education (LPDP) [00338/J5.2.3./BPI.06/9/2022].

DECLARATION OF GENERATIVE AI

Not applicable.

REFERENCES

[1] R. E. Vickman, O. E. Franco, D. C. Moline, D. J. Vander Griend, P. Thumbikat, and S. W. Hayward. (2020). "The Role of the Androgen Receptor in Prostate Development and Benign Prostatic Hyperplasia: A Review". *Asian Journal of Urology.* **7** (3): 191-202. 10.1016/j.ajur.2019.10.003.

[2] J. C. Nickel, C. G. Roehrborn, R. Castro-Santamaria, S. J. Freedland, and D. M. Moreira. (2016). "Chronic Prostate Inflammation Is Associated With Severity and Progression of Benign Prostatic Hyperplasia, Lower Urinary Tract Symptoms and Risk of Acute Urinary Retention". *The Journal of Urology.* **196** (5): 1493-1498. 10.1016/j.juro.2016.06.090.

[3] K. B. Lim. (2017). "Epidemiology of Clinical Benign Prostatic Hyperplasia". *Asian Journal of Urology.* **4** (3): 148-151. 10.1016/j.ajur.2017.06.004.

[4] R. Shukla, V. Pandey, G. P. Vadnere, and S. Lodhi. (2019). In: "Bioactive Food as Dietary Interventions for Arthritis and Related Inflammatory Diseases (Second Edition)". Elsevier. 10.1016/B978-0-12-813820-5.00018-0.

[5] O. Edirisinghe, G. Ternier, Z. Alraawi, and T. K. Suresh Kumar. (2024). "Decoding FGF/FGFR Signaling: Insights into Biological Functions and Disease Relevance". *Biomolecules.* **14** (12. 10.3390/biom14121622.

[6] G. Lee, H. Lee, L. Zhao, M. M. U. Rashid, M. K. Kim, Y. B. Jeong, H. Chae, and Y. S. Shin. (2023). "The Role of Reactive Oxygen Species, Inflammation, and Endoplasmic Reticulum Stress Response in the Finasteride Protective Effect Against Benign Prostate Hyperplasia". *World Journal of Men's Health.* **41** (3): 600-609. 10.5534/wjmh.230122.

[7] H. Zhang, L. Yang, Q. Han, and W. Xu. (2022). "Antifibrotic Effects of Quercetin on TGF-β1-Induced Vocal Fold Fibroblasts". *American Journal of Translational Research.* **14** (12): 8552-8561.

[8] S. Ghafouri-Fard, F. A. Shabestari, S. Vaezi, A. Abak, H. Shoorei, A. Karimi, M. Taheri, and A. Basiri. (2021). "Emerging Impact of Quercetin in the Treatment of Prostate Cancer". *Biomedicine and Pharmacotherapy.* **138** : 111548. 10.1016/j.biopha.2021.111548.

[9] M. Rafi, F. Hayati, A. H. Umar, D. A. Septaningsih, and T. Rachmatiah. (2023). "LC-HRMS-Based Metabolomics to Evaluate the Phytochemical Profile and Antioxidant Capacity of Cosmos Caudatus With Different Extraction Methods and Solvents". *Arabian Journal of Chemistry.* **16** (9): 105065. 10.1016/j.arabjc.2023.105065.

[10] W. Fu, S. Chen, Z. Zhang, Y. Chen, X. You, and Q. Li. (2022). "Quercetin in Tonglong Qibi Decoction Ameliorates Testosterone-Induced Benign Prostatic Hyperplasia in Rats by Regulating Nrf2 Signalling Pathways and Oxidative Stress". *Andrologia.* **54** (9). 10.1111/and.14502.

[11] M. J. Lee, Y. Cho, Y. Hwang, Y. Jo, Y. Kim, S. H. Lee, and J. H. Lee. (2023). "Kaempferol Alleviates Mitochondrial Damage by Reducing Mitochondrial Reactive Oxygen Species Production in Lipopolysaccharide-Induced Prostate Organoids". *Foods.* **12** (20). 10.3390/foods12203836.

[12] R. W. Azzahra, N. Murdaya, A. A. Al Shofwan, E. Ramadan, and S. D. Utami. (2021). "Molecular Docking Senyawa Ekstrak Etanol Daun Kenikir (Cosmos Caudatus) Sebagai Inhibitor IL-6 Dalam Respon Inflamasi". *Jurnal Farmasi Udayana.* **10** (2): 138. 10.24843/JFU.2021.v10.i02.p05.

[13] B. R. Jin, H. J. Kim, J. H. Na, W. K. Lee, and H. J. An. (2024). "Targeting Benign Prostate Hyperplasia Treatments: AR/TGF-β/NOX4 Inhibition by Apocynin Suppresses

Inflammation and Proliferation". *Journal of Advanced Research.* **57** : 135-147. 10.1016/j.jare.2023.04.006.

[14] A. Almatroudi, K. S. Allemailem, W. M. Alwanian, B. F. Alharbi, F. Alrumaihi, A. A. Khan, S. A. Almatroodi, and A. H. Rahmani. (2023). "Effects and Mechanisms of Kaempferol in the Management of Cancers Through Modulation of Inflammation and Signal Transduction Pathways". *International Journal of Molecular Sciences.* **24** (10). 10.3390/ijms24108630.

[15] Z. K. Tuong, K. W. Loudon, B. Berry, N. Richoz, J. Jones, X. Tan, Q. Nguyen, A. George, S. Hori, S. Field, A. G. Lynch, K. Kania, P. Coupland, A. Babbage, R. Grenfell, T. Barrett, A. Y. Warren, V. Gnanapragasam, C. Massie, and M. R. Clatworthy. (2021). "Resolving the Immune Landscape of Human Prostate at a Single-Cell Level in Health and Cancer". *Cell Reports.* **37** (12): 110132. 10.1016/j.celrep.2021.110132.

[16] D. Daud, N. F. Mohd Fekery, and N. Hashim. (2017). "Reproductive Health of Rats with Benign Prostatic Hyperplasia Following Cosmos Caudatus Ethanolic Extract Consumption". *Journal of Applied Pharmaceutical Science.* **7** (6): 202-205. 10.7324/JAPS.2017.70630.

[17] S. M. Lee, S. M. Lee, and J. Song. (2024). "Effects of Taraxaci Herba (Dandelion) on Testosterone Propionate-Induced Benign Prostatic Hyperplasia in Rats". *Nutrients.* **16** (8). 10.3390/nu16081189.

[18] S. Wang, Y. Li, W. Li, K. Zhang, Z. Yuan, Y. Cai, K. Xu, J. Zhou, and Z. Du. (2021). "Curcuma Oil Ameliorates Benign Prostatic Hyperplasia Through Suppression of the Nuclear Factor-Kappa B Signaling Pathway in Rats". *Journal of Ethnopharmacology.* **279** : 113703. 10.1016/j.jep.2020.113703.

[19] D. Nguyen, P. Herzog, E. B. Cone, M. Labban, K. C. Zorn, B. Chughtai, S. Basaria, D. S. Elterman, Q. Trinh, and N. Bhojani. (2023). "Disproportional Signal of Sexual Dysfunction Reports Associated with Finasteride Use in Young Men with Androgenetic Alopecia: A Pharmacovigilance Analysis of VigiBase". *Journal of the American Academy of Dermatology.* **88** (1): 179-181. 10.1016/j.jaad.2022.03.037.

[20] S. Madersbacher, N. Sampson, and Z. Culig. (2019). "Pathophysiology of Benign Prostatic Hyperplasia and Benign Prostatic Enlargement: A Mini-Review". *Gerontology.* **65** (5): 458-464. 10.1159/000496289.

[21] P. J. Espitia-Perez, L. M. Espitia-Perez, and M. Negrette-Guzman. (2025). "Targeting Prostate Cancer Metabolism Through Transcriptional and Epigenetic Modulation: A Multi-Target Approach to Therapeutic Innovation". *International Journal of Molecular Sciences.* **26** (13). 10.3390/ijms26136013.

[22] X. Wang, J. Zhu, H. Yan, M. Shi, Q. Zheng, Y. Wang, Y. Zhu, L. Miao, and X. Gao. (2021). "Kaempferol Inhibits Benign Prostatic Hyperplasia by Resisting the Action of Androgen". *European Journal of Pharmacology.* **893** : 173852. 10.1016/j.ejphar.2021.174251.

[23] L. V. Stewart and E. D. Lephart. (2023). "Androgen, Inflammation, and Growth Factor Interactions in the Progression of Benign Prostatic Hyperplasia". *Andrology.* **11** (2): 215-227. 10.1111/andr.13345.

[24] A. Khan, H. A. Alzahrani, S. G. Felemban, A. S. Algarni, A. B. S. Alenezi, M. Kamal, Z. U. Rehman, S. M. B. Asdaq, N. Ahmed, B. M. Alharbi, B. S. Alanazi, and M. Imran. (2025). "Exploring TGF-beta signaling in benign prostatic hyperplasia: from cellular senescence to fibrosis and therapeutic implications". *Biogerontology.* **26** (2): 79. 10.1007/s10522-025-10226-x.

[25] S. Halder, G. Brahmachari, and K. Jana. (2025). In: "Discovery and Development of Anti-Prostate Cancerous Agents from Natural Products". 9-35. 10.1016/b978-0-443-21842-2.00002-4.